

Category: Subsurface Hydrology

Analytical Solutions of Statistical Moments for
Transient Flow in Two-Dimensional Bounded,
Randomly Heterogeneous Media

Zhiming Lu and Dongxiao Zhang

Hydrology, Geochemistry, and Geology Group (EES-6)
MS T003, Los Alamos National Laboratory
Los Alamos, NM 87545

For Submission to *Water Resources Research*

June 3, 2004

ABSTRACT

In this paper, we derive analytical solutions of statistical moments for transient saturated flow in two-dimensional bounded, randomly heterogeneous porous media. By perturbation expansions, we first derive partial differential equations governing the zeroth-order head $h^{(0)}$ and the first-order head term $h^{(1)}$, where orders are in terms of the standard deviation of the log transmissivity. We then solve $h^{(0)}$ and $h^{(1)}$ analytically, both of which are expressed as infinite series. The head perturbation $h^{(1)}$ is then used to derive expressions for autocovariance of the hydraulic head and the cross-covariance between the log transmissivity and head. The expressions for the mean flux and flux covariance tensor are formulated from the head moments, based on Darcy's law. Using numerical examples, we demonstrate the convergence of these solutions. We also examine the accuracy of these first-order solutions by comparing them with solutions from both Monte Carlo simulations and the numerical moment-equation method.

INDEX TERMS: 1829 Hydrology: Groundwater Hydrology; 1832 Hydrology: Groundwater Transport; 1869 Hydrology: Stochastic Processes; 3210 Mathematical Geophysics: Modeling; 3230 Mathematical Geophysics: Numerical Solutions; *KEYWORDS:* stochastic processes, analytical solutions, heterogeneity, head covariance, velocity covariance, uncertainty quantification

1 Introduction

Geological formations are inherently heterogeneous and exhibit a high degree of variability in medium properties such as hydraulic conductivity and porosity. Medium heterogeneity has significant impacts on fluid flow and solute transport in the subsurface. Although these formations are intrinsically deterministic, we usually have incomplete knowledge on their properties. As a result, it is common to treat the medium properties as stochastic processes and solve the flow and transport problems in randomly heterogeneous media in a stochastic framework. In the last two decades, many stochastic theories have been developed to obtain the statistical moments for fluid flow and solute transport in such heterogeneous media [e.g., Freeze, 1975; Gelhar and Axness, 1983; Dagan, 1979, 1982, 1989; Graham and McLaughlin, 1989; Rubin, 1990; Gelhar, 1993; Shvidler, 1993; Cushman and Ginn, 1993; Osnes, 1995, 1998; Guadagnini and Neuman, 1999a,b]. Most of these theories resort to solving the original or moment equations numerically.

Analytical solutions to the statistical moments of saturated flow are only available for some special cases such as steady state uniform mean flow in an unbounded domain [Dagan, 1985; Gelhar, 1993; Rubin, 1990; Rubin and Dagan, 1992; Zhang and Neuman, 1992] and steady state uniform mean flow in a rectangular domain [Osnes, 1995, 1996]. Under the assumption of steady state uniform mean flow in an infinite domain, Dagan [1985] derived an analytical solution for the head variogram with an exponential covariance function of the log hydraulic conductivity. Under similar assumptions, Rubin and Dagan [1992] and Zhang and Neuman [1992] presented solutions to velocity covariances. Osnes [1995, 1998] derived analytical solutions to head and velocity moments for steady state uniform mean flow in a rectangular domain with a separable exponential covariance function of the log transmissivity. To our knowledge, analytical solutions for head and velocity moments for transient flow are not available in the literature. In this study, we present analytical solutions to head and velocity covariances for transient flow in a two-dimensional statistically homogeneous porous medium with a separable exponential covariance function of the log transmissivity. We assume that the boundary conditions are deterministic and the only source of uncertainty is due to the variability on transmissivity. It is also assumed that the flow is initially at a steady state condition and the initial head uncertainty is unknown (to be determined later)

rather than specified in advance.

2 Mathematical Derivation

2.1 Statement of the Problem

We consider transient flow in saturated two-dimensional bounded randomly heterogeneous porous media governed by the following continuity equation and Darcy's law

$$\nabla \cdot \mathbf{q}(\mathbf{x}, t) = S \frac{\partial h(\mathbf{x}, t)}{\partial t}, \quad \mathbf{x} \in \Omega, t > 0 \quad (1)$$

$$\mathbf{q}(\mathbf{x}, t) = -T(\mathbf{x}) \nabla h(\mathbf{x}, t) \quad (2)$$

with boundary and initial conditions

$$h(\mathbf{x}, t) = H_1, \quad x_1 = 0, \quad t > 0, \quad (3a)$$

$$h(\mathbf{x}, t) = H_2, \quad x_1 = L_1, \quad t > 0, \quad (3b)$$

$$\partial h(\mathbf{x}, t) / \partial x_2 = 0, \quad x_2 = 0, \quad t > 0, \quad (3c)$$

$$\partial h(\mathbf{x}, t) / \partial x_2 = 0, \quad x_2 = L_2, \quad t > 0, \quad (3d)$$

$$h(\mathbf{x}, t) = H_0(\mathbf{x}), \quad \mathbf{x} \in \Omega, \quad t = 0, \quad (3e)$$

where $h(\mathbf{x}, t)$ is the hydraulic head, $q(\mathbf{x}, t)$ is the specific discharge, H_1 and H_2 are prescribed constant heads, $H_0(\mathbf{x})$ is the initial head in the domain Ω , T is the transmissivity, S is storativity, $\mathbf{x} = (x_1, x_2)$ is the horizontal Cartesian coordinates, L_1 and L_2 are the lengths of the flow domain in x_1 and x_2 directions, and t is time. Here we assume that H_1 and H_2 are deterministic constants while $H_0(\mathbf{x})$ is specified with uncertainty: $H_0(\mathbf{x}) = \langle H_0(\mathbf{x}) \rangle + H'_0(\mathbf{x})$ where $\langle H_0 \rangle$ and $H'_0(\mathbf{x})$ are respectively the mean and perturbation. It is also assumed that S is a deterministic constant whereas T is a spatially correlated stationary random function following a log normal distribution, and we work with the log-transformed variable $Y(\mathbf{x}) = \ln[T(\mathbf{x})] = \langle Y \rangle + Y'(\mathbf{x})$, where $\langle Y \rangle$ and $Y'(\mathbf{x})$ are the mean and the perturbation of log transmissivity, respectively. Accordingly, the hydraulic head and flux are also random functions and can be decomposed as $h(\mathbf{x}, t) = h^{(0)}(\mathbf{x}, t) + h^{(1)}(\mathbf{x}, t) + \dots$, $\mathbf{q}(\mathbf{x}, t) = \mathbf{q}^{(0)}(\mathbf{x}, t) + \mathbf{q}^{(1)}(\mathbf{x}, t) + \dots$, where the order of each term in this series is in terms of the variability of the log transmissivity. Our aim is to solve for the statistics (mean and covariance) of head and flux.

2.2 First-order Mean Head and Mean Flux

Upon combining (1) and (2), substituting decompositions of $h(\mathbf{x}, t)$, $H_0(\mathbf{x})$, and $T(\mathbf{x}) = \exp(Y(\mathbf{x})) \approx T_G[1 + Y'(\mathbf{x})]$, where T_G is the geometric mean of transmissivity, into the derived equation with boundary and initial conditions (3), and collecting terms at zeroth order, one obtains the the following equation

$$\frac{\partial^2 h^{(0)}(\mathbf{x}, t)}{\partial x_1^2} + \frac{\partial^2 h^{(0)}(\mathbf{x}, t)}{\partial x_2^2} = \frac{S}{T_G} \frac{\partial h^{(0)}(\mathbf{x}, t)}{\partial t}, \quad \mathbf{x} \in \Omega, \quad t > 0 \quad (4)$$

with boundary and initial conditions

$$h^{(0)}(\mathbf{x}, t) = H_1, \quad x_1 = 0, \quad t > 0, \quad (5a)$$

$$h^{(0)}(\mathbf{x}, t) = H_2, \quad x_1 = L_1, \quad t > 0, \quad (5b)$$

$$\partial h^{(0)}(\mathbf{x}, t)/\partial x_2 = 0, \quad x_2 = 0, \quad t > 0, \quad (5c)$$

$$\partial h^{(0)}(\mathbf{x}, t)/\partial x_2 = 0, \quad x_2 = L_2, \quad t > 0, \quad (5d)$$

$$h^{(0)}(\mathbf{x}, 0) = \langle H_0(\mathbf{x}) \rangle, \quad \mathbf{x} \in \Omega. \quad (5e)$$

Certainly, the first-order transient mean head depends on the initial mean head. Here we choose a special case: $\langle H_0(\mathbf{x}) \rangle = H_{10} + (H_{20} - H_{10})x_1/L_1$, i.e., assuming a steady state initial condition with initial gradient of $J_0 = (H_{10} - H_{20})/L_1$. At time $t = 0$, the head values at two constant head boundaries are changed to H_1 and H_2 , respectively. The solution of (4)-(5) for such a scenario can be expressed as an infinite series (Appendix A):

$$h^{(0)}(\mathbf{x}, t) = \frac{2}{L_1} \sum_{m=1}^{\infty} \frac{\sin(\alpha_m x_1)}{\alpha_m} \left[(H_{10} - (-1)^m H_{20}) e^{-\frac{T_G}{S} \alpha_m^2 t} + (H_1 - (-1)^m H_2) \left(1 - e^{-\frac{T_G}{S} \alpha_m^2 t} \right) \right] \quad (6)$$

where $\alpha_m = m\pi/L_1$, $m = 1, 2, \dots$. Each term in this series is a weighted average of the effect of the constant head boundaries at time $t = 0$ and $t > 0$. Utilizing the identities $\sum_{k=1}^{\infty} \sin(kz)/k = (\pi - z)/2$ for $0 < z < 2\pi$ and $\sum_{k=1}^{\infty} (-1)^{k-1} \sin(kz)/k = z/2$ for $-\pi < z < \pi$, it can be verified that for $t = 0$ and $t = \infty$, (6) reduces to $h^{(0)}(\mathbf{x}, 0) = H_{10} + (H_{20} - H_{10})x_1/L_1$ and $h^{(0)}(\mathbf{x}, \infty) = H_1 + (H_2 - H_1)x_1/L_1$. For any time $0 < t < \infty$, $h^{(0)}(\mathbf{x}, t)$ has to be evaluated numerically. Since $\sin(\alpha_m x_1) = 0$ at two constant head boundaries $x_1 = 0$ and $x_1 = L_1$, the value of any truncated finite summation of (6) at these two constant head

boundaries will be zero. To avoid this, we may rewrite (6) in an alternative form:

$$h^{(0)}(\mathbf{x}, t) = H_1 + \frac{H_2 - H_1}{L_1} x_1 + \frac{2}{L_1} \sum_{m=1}^{\infty} \frac{b_m \sin(\alpha_m x_1)}{\alpha_m} e^{-\frac{T_G}{S} \alpha_m^2 t}, \quad (7)$$

where $b_m = (H_{10} - H_1) - (-1)^m (H_{20} - H_2)$. Similarly, after substituting decompositions of $\mathbf{q}(\mathbf{x}, t)$, $h(\mathbf{x}, t)$, and $Y(\mathbf{x})$ into (2) and collecting terms at the zeroth order, one has

$$\mathbf{q}^{(0)}(\mathbf{x}, t) = -T_G \nabla h^{(0)}(\mathbf{x}, t), \quad (8)$$

or, by utilizing (7), one has the following expressions for the flux components:

$$\begin{aligned} q_1^{(0)}(\mathbf{x}, t) &= T_G \left[J_1 - \frac{2}{L_1} \sum_{m=1}^{\infty} b_m \cos(\alpha_m x_1) e^{-\frac{T_G}{S} \alpha_m^2 t} \right] \\ q_2^{(0)}(\mathbf{x}, t) &= 0 \end{aligned} \quad (9)$$

where $J_1 = (H_1 - H_2)/L_1$ is the final steady state mean hydraulic gradient.

2.3 First-order Head Perturbations

The equation for the first-order term $h^{(1)}$ reads:

$$\frac{\partial^2 h^{(1)}(\mathbf{x}, t)}{\partial x_i^2} + \frac{\partial}{\partial x_i} \left(Y'(\mathbf{x}) \frac{\partial h^{(1)}(\mathbf{x})}{\partial x_i} \right) = \frac{S}{T_G} \frac{\partial h^{(1)}(\mathbf{x}, t)}{\partial t}, \quad \mathbf{x} \in \Omega, \quad t > 0 \quad (10)$$

where summation over repeated index is implied. Boundary and initial conditions corresponding to (10) are

$$h^{(1)}(\mathbf{x}, t) = 0, \quad x_1 = 0 \quad \text{or} \quad x_1 = L_1, \quad t > 0, \quad (11a)$$

$$\partial h^{(1)}(\mathbf{x}, t) / \partial x_2 = 0, \quad x_2 = 0 \quad \text{or} \quad x_2 = L_2, \quad t > 0, \quad (11b)$$

$$h^{(1)}(\mathbf{x}, 0) = H'_0(\mathbf{x}) \quad \mathbf{x} \in \Omega \quad (11c)$$

We have to emphasize that the perturbation of the initial head $H'_0(\mathbf{x})$ depends on the variability of $Y(\mathbf{x})$ and therefore cannot be arbitrarily assigned. By assuming that the flow system is initially at a steady state condition, the functional form of the unknown initial perturbation can be determined later. Equations (10)-(11) can be solved analytically (Appendix

B) and the solution is:

$$\begin{aligned}
& h^{(1)}(\mathbf{x}, t) \\
&= \frac{4}{D} \sum_{\substack{m=1 \\ n=0}}^{\infty} a_n \sin(\alpha_m x_1) \cos(\beta_n x_2) e^{-\frac{T_G}{S}(\alpha_m^2 + \beta_n^2)t} \int_{\Omega} H'_0(\mathbf{x}') \sin(\alpha_m x'_1) \cos(\beta_n x'_2) d\mathbf{x}' \\
&+ \frac{4J_1}{D} \sum_{\substack{m=1 \\ n=0}}^{\infty} \frac{a_n \alpha_m \sin(\alpha_m x_1) \cos(\beta_n x_2)}{\alpha_m^2 + \beta_n^2} \left[1 - e^{-\frac{T_G}{S}(\alpha_m^2 + \beta_n^2)t} \right] \int_{\Omega} Y'(\mathbf{x}') \cos(\alpha_m x'_1) \cos(\beta_n x'_2) d\mathbf{x}' \\
&- \frac{8T_G}{DL_1 S} \sum_{\substack{m,k=1 \\ n=0}}^{\infty} a_n b_k P_{kmn}(t) \alpha_m \sin(\alpha_m x_1) \cos(\beta_n x_2) \int_{\Omega} Y'(\mathbf{x}') \cos(\alpha_m x'_1) \cos(\alpha_k x'_1) \cos(\beta_n x'_2) d\mathbf{x}'
\end{aligned} \tag{12}$$

where $\beta_n = n\pi/L_2$, $n = 0, 1, 2, \dots$, $a_n = 1$ for $n > 0$ and $a_n = 1/2$ for $n = 0$, terms b_k and $P_{kmn}(t)$ are defined in Appendix B. Since $P_{kmn}(0) = 0$, it can be verified that $h^{(1)}(\mathbf{x}, 0) = H'(\mathbf{x})$. Note that $H'_0(\mathbf{x})$ depends only on $Y'(\mathbf{x})$, and so does the head perturbation $h^{(1)}(\mathbf{x}, t)$. By taking the limit of (12) as $t \rightarrow \infty$, one obtains the steady state solution of the head perturbation

$$h^{(1)}(\mathbf{x}, \infty) = \frac{4J_1}{D} \sum_{\substack{m=1 \\ n=0}}^{\infty} \frac{a_n \alpha_m \sin(\alpha_m x_1) \cos(\beta_n x_2)}{\alpha_m^2 + \beta_n^2} \int_{\Omega} Y'(\mathbf{x}') \cos(\alpha_m x'_1) \cos(\beta_n x'_2) d\mathbf{x}' \tag{13}$$

In particular, the initial head perturbation $H'_0(\mathbf{x})$ can be written as

$$H'_0(\mathbf{x}) = \frac{4J_0}{D} \sum_{\substack{m=1 \\ n=0}}^{\infty} \frac{a_n \alpha_m \sin(\alpha_m x_1) \cos(\beta_n x_2)}{\alpha_m^2 + \beta_n^2} \int_{\Omega} Y'(\mathbf{x}') \cos(\alpha_m x'_1) \cos(\beta_n x'_2) d\mathbf{x}', \tag{14}$$

which will be used to formulate the (cross-)covariance C_{YH_0} and C_{H_0} that are required in solving for transient head covariances.

2.4 Steady State Second Moments of Head

The cross-covariance between the log transmissivity and the steady state hydraulic head can be obtained by writing (13) in terms of (\mathbf{y}, τ) , multiplying $Y'(\mathbf{x})$ to the resulted equation, and taking the mean,

$$C_{Yh}(\mathbf{x}, \mathbf{y}) = \langle Y'(\mathbf{x}) h^{(1)}(\mathbf{y}, \infty) \rangle = \frac{4J_1}{D} \sum_{\substack{m=1 \\ n=0}}^{\infty} \frac{a_n \alpha_m \sin(\alpha_m y_1) \cos(\beta_n y_2)}{\alpha_m^2 + \beta_n^2} R_{mn}(\mathbf{x}), \tag{15}$$

where $R_{mn}(\mathbf{x}) = \int_{\Omega} C_Y(\mathbf{x}, \mathbf{x}') \cos(\alpha_m x'_1) \cos(\beta_n x'_2) d\mathbf{x}'$, and $C_Y(\mathbf{x}, \mathbf{x}') = \langle Y'(\mathbf{x}) Y'(\mathbf{x}') \rangle$ is the covariance of the log transmissivity Y . As done by Osnes [1995] and Yubin and Dagan [1988], we choose C_Y as a separable exponential function

$$C_Y(\mathbf{x}, \mathbf{x}') = \sigma_Y^2 \exp \left(-\frac{|x_1 - x'_1|}{\lambda_1} - \frac{|x_2 - x'_2|}{\lambda_2} \right), \quad (16)$$

where σ_Y^2 is the variance of Y , and λ_1 and λ_2 are the correlation lengths of Y in x_1 and x_2 directions, respectively. For this particular covariance function, $R_{mn}(\mathbf{x})$ can be found analytically:

$$R_{mn}(\mathbf{x}) = \frac{\lambda_1 \lambda_2 \sigma_Y^2}{(\alpha_m^2 \lambda_1^2 + 1)(\beta_n^2 \lambda_2^2 + 1)} \left[2 \cos(\alpha_m x_1) - e^{-x_1/\lambda_1} - (-1)^m e^{(x_1 - L_1)/\lambda_1} \right] \times \left[2 \cos(\beta_n x_2) - e^{-x_2/\lambda_2} - (-1)^n e^{(x_2 - L_2)/\lambda_2} \right] \quad (17)$$

The steady state head covariance can be derived by multiplying $h^{(1)}(\mathbf{y}, \infty)$ to (13), taking the mean, and substituting (15) into the derived equation,

$$C_h(\mathbf{x}, \mathbf{y}) = \frac{16J_1^2}{D^2} \sum_{\substack{m, m_1=1 \\ n, n_1=0}}^{\infty} \frac{a_n a_{n_1} \alpha_m \alpha_{m_1} \sin(\alpha_m x_1) \cos(\beta_n x_2) \sin(\alpha_{m_1} y_1) \cos(\beta_{n_1} y_2)}{(\alpha_m^2 + \beta_n^2)(\alpha_{m_1}^2 + \beta_{n_1}^2)} Q_{m_1 n_1}^{mn}, \quad (18)$$

where

$$Q_{m_1 n_1}^{mn} = \int_{\Omega} R_{m_1 n_1}(\mathbf{x}') \cos(\alpha_m x'_1) \cos(\beta_n x'_2) d\mathbf{x}' \\ = \frac{\lambda_1 \lambda_2 \sigma_Y^2}{(\alpha_{m_1}^2 \lambda_1^2 + 1)(\beta_{n_1}^2 \lambda_2^2 + 1)} \left[L_1 \delta_{mm_1} + \frac{\lambda_1}{\alpha_m^2 \lambda_1^2 + 1} [1 + (-1)^{m+m_1}] [(-1)^m e^{-L_1/\lambda_1} - 1] \right] \\ \left[(\delta_{nn_1} + \delta_{n0} \delta_{n_1 0}) L_2 + \frac{\lambda_2}{\beta_n^2 \lambda_2^2 + 1} [1 + (-1)^{n+n_1}] [(-1)^n e^{-L_2/\lambda_2} - 1] \right], \quad (19)$$

and δ_{ij} is the Kronecker delta function.

Equation (18) leads to the steady state head variance

$$\sigma_h^2(\mathbf{x}) = \frac{16J_1^2}{D^2} \sum_{\substack{m, m_1=1 \\ n, n_1=0}}^{\infty} \frac{a_n a_{n_1} \alpha_m \alpha_{m_1} \sin(\alpha_m x_1) \cos(\beta_n x_2) \sin(\alpha_{m_1} x_1) \cos(\beta_{n_1} x_2)}{(\alpha_m^2 + \beta_n^2)(\alpha_{m_1}^2 + \beta_{n_1}^2)} Q_{m_1 n_1}^{mn}. \quad (20)$$

Certainly, the expressions for the head covariance and head variance, i.e., (18) and (20), are much simpler than those of Osnes [1995, (14)-(15)]. Note that the expressions for the cross-covariance $\langle Y'(\mathbf{x}) H'_0(\mathbf{y}) \rangle$ and auto-covariance $C_{H_0}(\mathbf{x}, \mathbf{y})$ can be written similarly as (15) and (18), simply replacing J_1 in these equations by the initial hydraulic gradient J_0 .

2.5 Transient Second Moments of Head

The transient cross-covariance $C_{Yh}(\mathbf{x}; \mathbf{y}, \tau)$ and $C_h(\mathbf{x}, t; \mathbf{y}, \tau)$ can be derived from (12) as (see Appendix C)

$$\begin{aligned} C_{Yh}(\mathbf{x}; \mathbf{y}, \tau) &= \frac{4}{D} \sum_{\substack{m=1 \\ n=0}}^{\infty} \frac{a_n \alpha_m \sin(\alpha_m y_1) \cos(\beta_n y_2)}{\alpha_m^2 + \beta_n^2} R_{mn}(\mathbf{x}) J_{mn}(\tau) \\ &- \frac{8T_G}{DL_1 S} \sum_{\substack{m,k=1 \\ n=0}}^{\infty} a_n b_k P_{kmn}(\tau) \alpha_m \sin(\alpha_m y_1) \cos(\beta_n y_2) R_{kmn}(\mathbf{x}) \end{aligned} \quad (21)$$

$$\begin{aligned} C_h(\mathbf{x}, t; \mathbf{y}, \tau) &= \frac{16}{D^2} \sum_{\substack{m,m_1=1 \\ n,n_1=0}}^{\infty} \frac{a_n a_{n_1} \alpha_m \alpha_{m_1} Q_{mn}^{m_1 n_1} SC}{(\alpha_m^2 + \beta_n^2)(\alpha_{m_1}^2 + \beta_{n_1}^2)} J_{mn}(t) J_{m_1 n_1}(\tau) \\ &- \frac{32T_G}{D^2 L_1 S} \sum_{\substack{m,m_1,k_1=1 \\ n,n_1=0}}^{\infty} \frac{a_n a_{n_1} \alpha_m \alpha_{m_1} b_{k_1} P_{k_1 m_1 n_1}(\tau) SC}{\alpha_m^2 + \beta_n^2} Q_{mn}^{k_1 m_1 n_1} J_{mn}(t) \\ &- \frac{32T_G}{D^2 L_1 S} \sum_{\substack{m,m_1,k=1 \\ n,n_1=0}}^{\infty} \frac{a_n a_{n_1} \alpha_m \alpha_{m_1} b_k P_{kmn}(t) SC}{\alpha_{m_1}^2 + \beta_{n_1}^2} Q_{m_1 n_1}^{kmn} J_{m_1 n_1}(\tau) \\ &+ \frac{64T_G^2}{D^2 L_1^2 S^2} \sum_{\substack{m,m_1,k,k_1=1 \\ n,n_1=0}}^{\infty} a_n a_{n_1} \alpha_m \alpha_{m_1} b_k b_{k_1} P_{kmn}(t) P_{k_1 m_1 n_1}(\tau) SC Q_{kmn}^{k_1 m_1 n_1} \end{aligned} \quad (22)$$

where

$$SC = \sin(\alpha_m y_1) \cos(\beta_n y_2) \sin(\alpha_{m_1} x_1) \cos(\beta_{n_1} x_2), \quad (23)$$

$$J_{mn}(t) = \left[J_1 + (J_0 - J_1) e^{-\frac{T_G}{S}(\alpha_m^2 + \beta_n^2)t} \right], \quad (24)$$

and all other terms are given in Appendix C. By taking the limit as $t \rightarrow \infty$, (21) and (22) reduce to (15) and (18).

2.6 Second Moments of Flux

The first-order flux can be written as

$$\mathbf{q}^{(1)}(\mathbf{x}, t) = -T_G \nabla h^{(1)}(\mathbf{x}, t) + Y'(\mathbf{x}) \mathbf{q}^{(0)}(\mathbf{x}, t), \quad (25)$$

or in the component form:

$$q_i^{(1)}(\mathbf{x}, t) = -T_G \frac{\partial h^{(1)}(\mathbf{x}, t)}{\partial x_i} + Y'(\mathbf{x}) q_i^{(0)}(\mathbf{x}, t), \quad i = 1, 2. \quad (26)$$

Multiplying $Y'(\mathbf{y})$ on (26) and taking the mean yield

$$C_{Yq_i}(\mathbf{y}; \mathbf{x}, t) = \langle Y'(\mathbf{y}) q_i^{(1)}(\mathbf{x}, t) \rangle = -T_G \frac{\partial C_{Yh}(\mathbf{y}; \mathbf{x}, t)}{\partial x_i} + q_i^{(0)}(\mathbf{x}, t) C_Y(\mathbf{x}, \mathbf{y}). \quad (27)$$

More specifically, (27) can be expanded as

$$\begin{aligned} C_{Yq_1}(\mathbf{y}; \mathbf{x}, t) &= q_1^{(0)}(\mathbf{x}, t) C_Y(\mathbf{x}, \mathbf{y}) - \frac{4T_G}{D} \sum_{\substack{m=1 \\ n=0}}^{\infty} \frac{a_n \alpha_m^2 \cos(\alpha_m x_1) \cos(\beta_n x_2)}{\alpha_m^2 + \beta_n^2} R_{mn}(\mathbf{y}) J_{mn}(t) \\ &+ \frac{8T_G^2}{DL_1 S} \sum_{\substack{m,k=1 \\ n=0}}^{\infty} a_n b_k \alpha_m^2 P_{kmn}(t) \cos(\alpha_m x_1) \cos(\beta_n x_2) R_{kmn}(\mathbf{y}) \end{aligned} \quad (28)$$

and

$$\begin{aligned} C_{Yq_2}(\mathbf{y}; \mathbf{x}, t) &= \frac{4T_G}{D} \sum_{\substack{m=1 \\ n=0}}^{\infty} \frac{a_n \alpha_m \beta_n \sin(\alpha_m x_1) \sin(\beta_n x_2)}{\alpha_m^2 + \beta_n^2} R_{mn}(\mathbf{y}) J_{mn}(t) \\ &- \frac{8T_G^2}{DL_1 S} \sum_{\substack{m,k=1 \\ n=0}}^{\infty} a_n b_k \alpha_m \beta_n P_{kmn}(t) \sin(\alpha_m x_1) \sin(\beta_n x_2) R_{kmn}(\mathbf{y}) \end{aligned} \quad (29)$$

The flux covariance $q_{ij}(\mathbf{x}, t; \mathbf{y}, \tau) = \langle q_i^{(1)}(\mathbf{x}, t) q_j^{(1)}(\mathbf{y}, \tau) \rangle$ can be derived from (26)

$$\begin{aligned} q_{ij}(\mathbf{x}, t; \mathbf{y}, \tau) &= T_G^2 \frac{\partial^2 C_h(\mathbf{x}, t; \mathbf{y}, \tau)}{\partial x_i \partial y_j} - T_G q_j^{(0)}(\mathbf{y}, \tau) \frac{\partial C_{Yh}(\mathbf{y}; \mathbf{x}, t)}{\partial x_i} \\ &- T_G q_i^{(0)}(\mathbf{x}, t) \frac{\partial C_{Yh}(\mathbf{x}; \mathbf{y}, \tau)}{\partial y_j} + q_i^{(0)}(\mathbf{x}, t) q_j^{(0)}(\mathbf{y}, \tau) C_Y(\mathbf{x}, \mathbf{y}), i, j = 1, 2, \end{aligned} \quad (30)$$

which can be elaborated as

$$\begin{aligned}
q_{11}(\mathbf{x}, t; \mathbf{y}, \tau) &= \frac{16T_G^2}{D^2} \sum_{\substack{m, m_1=1 \\ n, n_1=0}}^{\infty} \frac{a_n a_{n_1} \alpha_m^2 \alpha_{m_1}^2 Q_{mn}^{m_1 n_1} CC}{(\alpha_m^2 + \beta_n^2)(\alpha_{m_1}^2 + \beta_{n_1}^2)} J_{mn}(t) J_{m_1 n_1}(\tau) \\
&- \frac{32T_G^3}{D^2 L_1 S} \sum_{\substack{m, m_1, k_1=1 \\ n, n_1=0}}^{\infty} \frac{a_n a_{n_1} \alpha_m^2 \alpha_{m_1}^2 b_{k_1} P_{k_1 m_1 n_1}(\tau) CC}{\alpha_m^2 + \beta_n^2} Q_{mn}^{k_1 m_1 n_1} J_{mn}(t) \\
&- \frac{32T_G^3}{D^2 L_1 S} \sum_{\substack{m, m_1, k=1 \\ n, n_1=0}}^{\infty} \frac{a_n a_{n_1} \alpha_m^2 \alpha_{m_1}^2 b_k P_{kmn}(t) CC}{\alpha_{m_1}^2 + \beta_{n_1}^2} Q_{m_1 n_1}^{kmn} J_{m_1 n_1}(\tau) \\
&+ \frac{64T_G^4}{D^2 L_1^2 S^2} \sum_{\substack{m, m_1, k, k_1=1 \\ n, n_1=0}}^{\infty} a_n a_{n_1} \alpha_m^2 \alpha_{m_1}^2 b_k b_{k_1} P_{kmn}(t) P_{k_1 m_1 n_1}(\tau) CC Q_{kmn}^{k_1 m_1 n_1} \\
&- \frac{4T_G q_1^{(0)}(\mathbf{y}, \tau)}{D} \sum_{\substack{m=1 \\ n=0}}^{\infty} \frac{a_n \alpha_m^2 \cos(\alpha_m x_1) \cos(\beta_n x_2)}{\alpha_m^2 + \beta_n^2} R_{mn}(\mathbf{y}) J_{mn}(t) \\
&+ \frac{8T_G^2 q_1^{(0)}(\mathbf{y}, \tau)}{DL_1 S} \sum_{\substack{m, k=1 \\ n=0}}^{\infty} a_n b_k P_{kmn}(t) \alpha_m^2 \cos(\alpha_m x_1) \cos(\beta_n x_2) R_{kmn}(\mathbf{y}) \\
&- \frac{4T_G q_1^{(0)}(\mathbf{x}, t)}{D} \sum_{\substack{m=1 \\ n=0}}^{\infty} \frac{a_n \alpha_m^2 \cos(\alpha_m y_1) \cos(\beta_n y_2)}{\alpha_m^2 + \beta_n^2} R_{mn}(\mathbf{x}) J_{mn}(\tau) \\
&+ \frac{8T_G^2 q_1^{(0)}(\mathbf{x}, t)}{DL_1 S} \sum_{\substack{m, k=1 \\ n=0}}^{\infty} a_n b_k P_{kmn}(\tau) \alpha_m^2 \cos(\alpha_m y_1) \cos(\beta_n y_2) R_{kmn}(\mathbf{x}) \\
&+ q_1^{(0)}(\mathbf{x}, t) q_1^{(0)}(\mathbf{y}, \tau) C_Y(\mathbf{x}, \mathbf{y})
\end{aligned} \tag{31}$$

$$\begin{aligned}
q_{12}(\mathbf{x}, t; \mathbf{y}, \tau) = & -\frac{16T_G^2}{D^2} \sum_{\substack{m, m_1=1 \\ n, n_1=0}}^{\infty} \frac{a_n a_{n_1} \alpha_m \alpha_{m_1}^2 \beta_n Q_{mn}^{m_1 n_1} SC}{(\alpha_m^2 + \beta_n^2)(\alpha_{m_1}^2 + \beta_{n_1}^2)} J_{mn}(t) J_{m_1 n_1}(\tau) \\
& + \frac{32T_G^3}{D^2 L_1 S} \sum_{\substack{m, m_1, k_1=1 \\ n, n_1=0}}^{\infty} \frac{a_n a_{n_1} \alpha_m \beta_n \alpha_{m_1}^2 b_{k_1} P_{k_1 m_1 n_1}(\tau) SC}{\alpha_m^2 + \beta_n^2} Q_{mn}^{k_1 m_1 n_1} J_{mn}(t) \\
& + \frac{32T_G^3}{D^2 L_1 S} \sum_{\substack{m, m_1, k=1 \\ n, n_1=0}}^{\infty} \frac{a_n a_{n_1} \alpha_m \alpha_{m_1}^2 \beta_n b_k P_{kmn}(t) SC}{\alpha_{m_1}^2 + \beta_{n_1}^2} Q_{m_1 n_1}^{kmn} J_{m_1 n_1}(\tau) \\
& - \frac{64T_G^4}{D^2 L_1^2 S^2} \sum_{\substack{m, m_1, k, k_1=1 \\ n, n_1=0}}^{\infty} a_n a_{n_1} \alpha_m \alpha_{m_1}^2 \beta_n b_k b_{k_1} P_{kmn}(t) P_{k_1 m_1 n_1}(\tau) SC Q_{kmn}^{k_1 m_1 n_1} \\
& + \frac{4T_G q_1^{(0)}(\mathbf{x}, t)}{D} \sum_{\substack{m=1 \\ n=0}}^{\infty} \frac{a_n \alpha_m \beta_n \sin(\alpha_m y_1) \sin(\beta_n y_2)}{\alpha_m^2 + \beta_n^2} R_{mn}(\mathbf{x}) J_{mn}(\tau) \\
& - \frac{8T_G^2 q_1^{(0)}(\mathbf{x}, t)}{DL_1 S} \sum_{\substack{m, k=1 \\ n=0}}^{\infty} a_n b_k P_{kmn}(\tau) \alpha_m \beta_n \sin(\alpha_m y_1) \sin(\beta_n y_2) R_{kmn}(\mathbf{x}) \quad (32)
\end{aligned}$$

and

$$\begin{aligned}
q_{22}(\mathbf{x}, t; \mathbf{y}, \tau) = & \frac{16T_G^2}{D^2} \sum_{\substack{m, m_1=1 \\ n, n_1=0}}^{\infty} \frac{a_n a_{n_1} \alpha_m \alpha_{m_1} \beta_n \beta_{n_1} Q_{mn}^{m_1 n_1} SS}{(\alpha_m^2 + \beta_n^2)(\alpha_{m_1}^2 + \beta_{n_1}^2)} J_{mn}(t) J_{m_1 n_1}(\tau) \\
& - \frac{32T_G^3}{D^2 L_1 S} \sum_{\substack{m, m_1, k_1=1 \\ n, n_1=0}}^{\infty} \frac{a_n a_{n_1} \alpha_m \alpha_{m_1} \beta_n \beta_{n_1} b_{k_1} P_{k_1 m_1 n_1}(\tau) SS}{\alpha_m^2 + \beta_n^2} Q_{mn}^{k_1 m_1 n_1} J_{mn}(t) \\
& - \frac{32T_G^3}{D^2 L_1 S} \sum_{\substack{m, m_1, k=1 \\ n, n_1=0}}^{\infty} \frac{a_n a_{n_1} \alpha_m \alpha_{m_1} \beta_n \beta_{n_1} b_k P_{kmn}(t) SS}{\alpha_{m_1}^2 + \beta_{n_1}^2} Q_{m_1 n_1}^{kmn} J_{m_1 n_1}(\tau) \\
& + \frac{64T_G^4}{D^2 L_1^2 S^2} \sum_{\substack{m, m_1, k, k_1=1 \\ n, n_1=0}}^{\infty} a_n a_{n_1} \alpha_m \alpha_{m_1} \beta_n \beta_{n_1} b_k b_{k_1} P_{kmn}(t) P_{k_1 m_1 n_1}(\tau) SS Q_{kmn}^{k_1 m_1 n_1} \quad (33)
\end{aligned}$$

where

$$\begin{aligned}
SC &= \sin(\alpha_m y_1) \sin(\beta_n y_2) \cos(\alpha_{m_1} x_1) \cos(\beta_{n_1} x_2), \\
CC &= \cos(\alpha_m y_1) \cos(\beta_n y_2) \cos(\alpha_{m_1} x_1) \cos(\beta_{n_1} x_2), \\
SS &= \sin(\alpha_m y_1) \sin(\beta_n y_2) \sin(\alpha_{m_1} x_1) \sin(\beta_{n_1} x_2). \quad (34)
\end{aligned}$$

The expression for q_{21} has been omitted, because of the fact $q_{21}(\mathbf{x}, t; \mathbf{y}, \tau) \equiv q_{12}(\mathbf{y}, \tau; \mathbf{x}, t)$. Since $q_1(\mathbf{x}, \infty) = T_G J_1$ and $J_{mn}(\infty) = J_1$, the steady state flux covariance can be written from (31)-(33) as

$$\begin{aligned}
q_{11}(\mathbf{x}; \mathbf{y}) &= \frac{16T_G^2 J_1^2}{D^2} \sum_{\substack{m, m_1=1 \\ n, n_1=0}}^{\infty} \frac{a_n a_{n_1} \alpha_m^2 \alpha_{m_1}^2 Q_{mn}^{m_1 n_1}}{(\alpha_m^2 + \beta_n^2)(\alpha_{m_1}^2 + \beta_{n_1}^2)} \cos(\alpha_m y_1) \cos(\beta_n y_2) \cos(\alpha_{m_1} x_1) \cos(\beta_{n_1} x_2) \\
&- \frac{4T_G^2 J_1^2}{D} \sum_{\substack{m=1 \\ n=0}}^{\infty} \frac{a_n \alpha_m^2}{\alpha_m^2 + \beta_n^2} [R_{mn}(\mathbf{x}) \cos(\alpha_m y_1) \cos(\beta_n y_2) + R_{mn}(\mathbf{y}) \cos(\alpha_m x_1) \cos(\beta_n x_2)] \\
&+ T_G^2 J_1^2 C_Y(\mathbf{x}, \mathbf{y})
\end{aligned} \tag{35}$$

$$\begin{aligned}
q_{12}(\mathbf{x}; \mathbf{y}) &= -\frac{16T_G^2 J_1^2}{D^2} \sum_{\substack{m, m_1=1 \\ n, n_1=0}}^{\infty} \frac{a_n a_{n_1} \alpha_m \alpha_{m_1}^2 \beta_n Q_{mn}^{m_1 n_1}}{(\alpha_m^2 + \beta_n^2)(\alpha_{m_1}^2 + \beta_{n_1}^2)} \sin(\alpha_m y_1) \sin(\beta_n y_2) \cos(\alpha_{m_1} x_1) \cos(\beta_{n_1} x_2) \\
&+ \frac{4T_G^2 J_1^2}{D} \sum_{\substack{m=1 \\ n=0}}^{\infty} \frac{a_n \alpha_m \beta_n \sin(\alpha_m y_1) \sin(\beta_n y_2)}{\alpha_m^2 + \beta_n^2} R_{mn}(\mathbf{x})
\end{aligned} \tag{36}$$

and

$$q_{22}(\mathbf{x}; \mathbf{y}) = \frac{16T_G^2 J_1^2}{D^2} \sum_{\substack{m, m_1=1 \\ n, n_1=0}}^{\infty} \frac{a_n a_{n_1} \alpha_m \alpha_{m_1} \beta_n \beta_{n_1} Q_{mn}^{m_1 n_1}}{(\alpha_m^2 + \beta_n^2)(\alpha_{m_1}^2 + \beta_{n_1}^2)} \sin(\alpha_m y_1) \sin(\beta_n y_2) \sin(\alpha_{m_1} x_1) \sin(\beta_{n_1} x_2) \tag{37}$$

The velocity covariance can be readily formulated from a simple relationship $u_{ij}(\mathbf{x}, t; \mathbf{y}, \tau) = q_{ij}(\mathbf{x}, t; \mathbf{y}, \tau)/\phi(\mathbf{x})/\phi(\mathbf{y})$, where ϕ is the porosity of the porous media and is considered as a deterministic quantity due to its relatively small variability.

3 Numerical Examples

In this section, we try to examine the convergence and the accuracy of the analytical solutions for the first-order transient mean flow quantities and related (cross-)covariances. We consider a two-dimensional rectangular domain in a saturated heterogeneous porous medium. The flow domain for our base case is a square of a size $L_1 = L_2 = 10$ (in any consistent length unit), uniformly discretized into 40×40 square elements. The non-flow conditions are prescribed at two lateral boundaries and constant heads are specified on the left and right

boundaries. Initially, the flow is at a steady state condition with constant heads $H_{10} = 9.5$ on the left boundary and $H_{20} = 9.0$ on the right boundary. At time $t = 0$, the constant heads on the left and right boundaries are suddenly changed to $H_1 = 11.0$ and $H_2 = 10.0$, respectively. The storativity is a deterministic constant $S = 0.005$. The mean of the log transmissivity is given as $\langle Y \rangle = 0.0$ (i.e., the geometric mean of transmissivity $T_G = 1.0$). The variance and the correlation lengths of the log transmissivity field for our base case are $\sigma_Y^2 = 1.0$ and $\lambda_1 = \lambda_2 = 1.0$. Unless specifically mentioned, in all examples we will show results only along the profile $x_2 = L_2/2 = 5$.

3.1 Convergence of Analytical Solutions

An important aspect of analytical solutions presented as infinity series is how fast the solutions converge to their true solutions, or in other words, how many terms should be included in truncating the series so that the approximations to these solutions will have a given accuracy. Many factors, including the aspect ratio of the flow domain and the correlation lengths of the log transmissivity field, may have impacts on the rate of convergence. To investigate this, in addition to the base case, we design two more cases. For each case, we truncate each individual summation (each index) in the analytical solutions of the mean head and the head variance up to N terms, where $N = 2, 3, 5, 6$, and 10 . Figure 1 illustrates the computed transient mean head at four times $t = 0.0, 0.01, 0.05$, and 0.4 , using $N = 2, 3$, and 5 . The figure shows that at time $t = 0.4$, the flow has reached the final steady state condition. From the figure we see that keeping the first two terms in the summation of $h^{(0)}(\mathbf{x})$ is very accurate, except for at early time $t = 0.01$, in which keeping the first-three terms is accurate enough. In all examples presented in this study, approximating the mean head with the first three terms in (7) is sufficiently accurate, and adding more terms does not significantly improve the accuracy. Mathematical analysis of the expression for $h^{(0)}(\mathbf{x})$, i.e., (7), reveals that for an extremely small t , a very large number of terms is needed. However, in general, the series in (7) converges very fast, and therefore, we will focus our discussion on the head variance. Figure 2 depicts the head variance as a function of x_1 along the profile $x_2 = L_2/2$ for different values of N . The figure clearly demonstrates that the rate of convergence depends on the flow condition. When the flow is close to a steady state condition, for instance at $t = 0.4$, approximating the head variance using $N = 3$ (i.e., 729 terms in a

six-fold summation) will be very accurate. While at early times, due to the sudden change on constant head boundary at $t = 0$, more terms are needed to approximating the head variance.

To examine the possible effect of the domain geometry (the ratio L_1/L_2) on the convergence of the solution, we change the width of the domain to $L_2 = 2$ while keeping everything else the same as in the base case. Numerical experiments with different numbers of terms included in the truncated summations are illustrated in Figure 3, which depicts the mean head and head variance along the profile $x_2 = L_2/2 = 1.0$. The figure, again, shows that the analytical solution converges faster when the flow is at or near a steady state condition. In addition, comparing Figures 2 and 3, one finds that the head variance increases as the domain becomes narrower in the transverse direction.

In the third example, we increase the correlation lengths of the log transmissivity to $\lambda_1 = \lambda_2 = 5$. The results, as shown in Figure 4, indicates that an increase of the correlation length enhances the rate of convergence of the analytical solution (compared to Fig. 2). Furthermore, it is seen that increases of the correlation lengths will cause an increase on the head variability. However, unlike the case with an unbounded domain with an exponential covariance function, the head variance here is not proportional to $\lambda_1 \lambda_2$.

3.2 Accuracy of Analytical Solutions

We conduct Monte Carlo (MC) simulations to verify the accuracy of the first-order analytical solutions for transient head and its related (cross-)covariances. First, we generate 5,000 two-dimensional unconditional realizations of the log transmissivity with the separable covariance function as given in (16), using the random field generator based on the Karhunen-Loève decomposition, as described in *Zhang and Lu* [2004]. The quality of these realizations has been examined by comparing their sample statistics (mean, variance, and correlation lengths) of these realizations with the specified mean and covariance functions. The comparisons show that the generated random fields reproduce the specified mean and covariance functions very well.

For each realization, we solve the steady-state flow equation with the initial constant head $H_{10} = 9.5$ and $H_{20} = 9.0$ on the left and the right boundaries, using the finite-element heat- and mass-transfer code (FEHM) of *Zyvoloski et al.* [1997]. This steady state head

field is then taken as the initial head $H_0(\mathbf{x})$ for the following transient simulation. Using the same realization, we run the FEHM code again for a transient simulation with the new constant heads $H_1 = 11.0$ and $H_2 = 10.0$ on the left and right boundaries and record the head at the following times: $t = 0, 0.01, 0.05$, and 0.4 . This procedure is repeated for all realizations, and the sample statistics of the transient flow fields, i.e., the mean predictions of the head and the flux as well as their (cross-)covariances at these times, are computed from realizations. These flow statistics are considered the “true” solutions that are used to evaluate the accuracy of the first-order analytical solutions.

Figure 5a compares the transient mean head $\langle h(\mathbf{x}, t) \rangle$ computed from Monte Carlo simulations (MC, solid curves) and that from the first-order (in σ_Y^2) analytical solution with $N = 10$ (ANA, dashed curves) at various times along the profile $x_2 = L_2/2$. It seems from the figure that the mean head computed from the analytical solution is very close to the Monte Carlo results, especially at or near steady state conditions. Also compared in the figure is the first-order mean head computed from the moment-equation method (ME, dash-dotted curves) [Zhang and Lu, 2002]. Figure 5b compares the transient head variance obtained from the MC simulations, the first-order analytical solution, and the first-order ME approach at various times. It is expected that the first-order analytical solutions should be identical to the results from the first-order ME method, in the limit that the number of terms, N , in the truncated finite series of the analytical solutions approaches to infinity. Furthermore, both first-order results will deviate slightly from the Monte Carlo results, and such deviations will increase with the increase of the variability of the log transmissivity. Figure 5 clearly shows that the analytical solutions are adequately accurate at $\sigma_Y^2 = 1.0$, especially when the flow is at or near a steady state condition.

It is interesting to see from Figure 5b that the head variance along the profile $x_2 = L_2/2$ at both the initial and final steady state conditions is symmetric (larger head variance at the final steady state condition due to a larger hydraulic gradient), while at any unsteady stage the curve is asymmetric. For example, the head variance along the profile has two peaks at time $t = 0.01$. This may be due to the variable hydraulic gradient during the unsteady stage. Comparison of Figure 5a and Figure 5b indicates that the larger peak on the variance curve corresponds to a larger hydraulic gradient on the mean head curve. Furthermore, because the change of the head variance from the initial head variance is due to the change

of constant head boundaries at $t = 0$, the variance change starts from two constant head boundaries and propagates into the entire flow domain. As a result, at a time before the effect of the boundary change reaches the entire domain, the head variance in some region remains the same as the initial head variance $\sigma_{H_0}^2(\mathbf{x})$ (e.g., a trough at $t = 0.01$ in Fig. 5b).

Figure 6a illustrates the cross-covariance $C_{Yh}(\mathbf{x}; \mathbf{x}, t)$ as a function of x_1 obtained from Monte Carlo simulations (solid curves) and analytical solutions (dashed curves) at four elapsed times. It is evident that analytical results are in good agreement with Monte Carlo results. Note that, at early time, $C_{Yh}(\mathbf{x}; \mathbf{x}, t)$ is much larger than its values at the steady state condition. This implies that at early time, the effect of the transmissivity is relatively local, i.e., the transmissivity at point \mathbf{x} has a significant effect on the mean head at the same point \mathbf{x} . Such an effect reduces significantly at later times because the transmissivity elsewhere in the domain also have impact on the mean head at point \mathbf{x} .

Figure 6b depicts the cross-covariance between the log transmissivity at the center of domain $(L_1/2, L_2/2)$ and the head $h(\mathbf{x}, t)$ along the profile $x_2 = L_2/2$, as a function of x_1 . Again, analytical results are in good agreement with Monte Carlo results. It is interesting to note that, at both the initial and the final steady state conditions, C_{Yh} along this profile is antisymmetric and $C_{Yh} = 0$ for Y and $h(\mathbf{x}, t)$ at the center of the domain, due to the particular boundary conditions in our problem. However, at any transient state, C_{Yh} does not shown any such kind of symmetry.

Figure 7 shows the covariance of head at $(x_1, L_2/2, t)$ and $(x_1, L_2/2, \tau)$ as a function of x_1 and τ at two different times $t = 0.00$ and $t = 0.05$, where solid curves stand for the results from Monte Carlo simulations and dashed curves from analytical solutions.

Comparison of the mean longitudinal flux obtained from the MC simulations, the analytical solution, and the ME method are illustrated in Figure 8, and similar comparisons for the flux variance are depicted in Figure 9, where the plots for a later time $t = 0.4$ are enlarged in inserts for a detail view. Clearly, Figures 8-9 once again demonstrate the accuracy of the analytical solutions. In addition, the transient flux variance could be significantly larger than the steady state flux variance.

3.3 Summary and Discussion

In this study, we derive analytical solutions of statistical moments (mean and covariance of both the hydraulic head and the flux) for transient saturated flow in two-dimensional bounded, randomly heterogeneous porous media, assuming that the flow is initially at a steady state condition. The initial steady state uncertainty on the head is determined rather than arbitrarily prescribed, under the assumption that the variability of the log hydraulic conductivity is the only source of uncertainty.

By perturbation expansions, we first derive partial differential equations governing the zeroth-order head $h^{(0)}$ and the first-order head term $h^{(1)}$, where orders are in terms of σ_Y , the standard deviation of the log transmissivity. We then solve $h^{(0)}$ and $h^{(1)}$ analytically, both of which are expressed as infinite series. The head perturbation $h^{(1)}$ is then used to derive expressions for auto-covariance of the hydraulic head and the cross-covariance between the log transmissivity and the head. Once the head moments are obtained, the expressions for the mean flux and flux covariance tensor are formulated, based on Darcy's law. The velocity covariance tensor could be computed readily from the flux covariance for a deterministic porosity.

We conducted numerical experiments to evaluate the convergence and the accuracy of the first-order analytical solutions. It has been shown that the rate of convergence depends on the flow condition, the aspect ratio of the flow domain (L_1/L_2), and the correlation lengths of the transmissivity. When the flow is at or near a steady state, the analytical solutions converge very fast, and for unsteady flow, more terms in the truncated finite series are required to approximate statistical moments. In addition, a large aspect ratio enhances the rate of convergence. Furthermore, large correlation lengths will also speed up the convergence. Finally, it seems that the solutions for the mean quantities converge faster do the solutions for the second moments.

We also examined the accuracy of these first-order analytical solutions by comparing them with solutions from both Monte Carlo simulations and the moment-equation method. The numerical experiments clearly show that the first-order analytical solutions are adequately accurate at least for $\sigma_Y^2 = 1.0$.

Appendix A: Zeroth-order Mean Head $h^{(0)}(\mathbf{x}, t)$

Here we briefly outline the procedure for solving the following equation for the zeroth-order mean head $h^{(0)}(\mathbf{x}, t)$,

$$\frac{\partial^2 h^{(0)}(\mathbf{x}, t)}{\partial x_1^2} + \frac{\partial^2 h^{(0)}(\mathbf{x}, t)}{\partial x_2^2} = \frac{S}{T_G} \frac{\partial h^{(0)}(\mathbf{x}, t)}{\partial t} \quad (\text{A1})$$

with boundary conditions and initial conditions, as shown in (5a)-(5e). Under the given boundary conditions, by using an integral transformation [Özişik, 1989]:

$$h^*(\alpha_m, \beta_n, t) = \int_{\Omega} K(\alpha_m, x_1) K(\beta_n, x_2) h^{(0)}(\mathbf{x}, t) d\mathbf{x}, \quad (\text{A2})$$

where kernels

$$K(\alpha_m, x_1) = \sqrt{\frac{2}{L_1}} \sin(\alpha_m x_1), \quad (\text{A3})$$

and

$$K(\beta_n, x_2) = \begin{cases} \sqrt{\frac{2}{L_2}} \cos(\beta_n x_2) & \text{if } n \neq 0, \\ \sqrt{\frac{1}{L_2}} & \text{if } n = 0, \end{cases} \quad (\text{A4})$$

and $\alpha_m = m\pi/L_1, m = 1, 2, \dots, \beta_n = n\pi/L_2, n = 0, 1, \dots$, (A1) is transformed to a first-order ordinary differential equation,

$$\frac{dh^*(\alpha_m, \beta_n, t)}{dt} + \frac{T_G}{S} (\alpha_m^2 + \beta_n^2) h^*(\alpha_m, \beta_n, t) = A(\alpha_m, \beta_n, t), \quad (\text{A5})$$

with the initial condition

$$F^*(\alpha_m, \beta_n) = \int_{\Omega} K(\alpha_m, x_1) K(\beta_n, x_2) \langle H_0(\mathbf{x}) \rangle d\mathbf{x} \quad (\text{A6})$$

which is the transformation of the initial condition (5e). The term on the right-hand side of (A5) is related to boundary conditions of the original zeroth-order equation,

$$\begin{aligned} A(\alpha_m, \beta_n, t) &= \frac{T_G}{S} \left[\frac{dK(\alpha_m, x_1)}{dx_1} \Big|_{x_1=0} \int_{x_2=0}^{L_2} K(\beta_n, x_2) H_1 dx_2 \right. \\ &\quad \left. + \frac{dK(\alpha_m, x_1)}{dx_1} \Big|_{x_1=L_1} \int_{x_2=0}^{L_2} K(\beta_n, x_2) H_2 dx_2 \right] \\ &= \begin{cases} 0 & \text{if } n \neq 0, \\ \frac{T_G}{S} \sqrt{\frac{2L_2}{L_1}} \alpha_m (H_1 - (-1)^m H_2) & \text{if } n = 0, \end{cases} \end{aligned} \quad (\text{A7})$$

Equation (A5) with the initial condition (A6) can be solved easily,

$$h^*(\alpha_m, \beta_n, t) = F^*(\alpha_m, \beta_n) + \int_{t'=0}^t e^{\frac{T_G}{S}(\alpha_m^2 + \beta_n^2)t'} A(\alpha_m, \beta_n, t') dt' \quad (\text{A8})$$

and the solution for $h^{(0)}(\mathbf{x}, t)$ can be derived from back-transformation of $h^*(\alpha_m, \beta_n, t)$,

$$\begin{aligned} h^{(0)}(\mathbf{x}, t) &= \sum_{m=1}^{\infty} \sum_{n=0}^{\infty} e^{-\frac{T_G}{S}(\alpha_m^2 + \beta_n^2)t} K(\alpha_m, x_1) K(\beta_n, x_2) h^*(\alpha_m, \beta_n, t) \\ &= \sum_{m=1}^{\infty} \sum_{n=0}^{\infty} e^{-\frac{T_G}{S}(\alpha_m^2 + \beta_n^2)t} K(\alpha_m, x_1) K(\beta_n, x_2) \int_{\Omega} K(\alpha_m, x'_1) K(\beta_n, x'_2) \langle H_0(\mathbf{x}') \rangle d\mathbf{x}' \\ &+ \frac{2}{L_1} \sum_{m=1}^{\infty} \frac{\sin(\alpha_m x_1)}{\alpha_m} (H_1 - (-1)^m H_2) \left(1 - e^{-\frac{T_G}{S}\alpha_m^2 t}\right). \end{aligned} \quad (\text{A9})$$

Assuming $\langle H_0(\mathbf{x}) \rangle = H_{10} + (H_{20} - H_{10}) x_1/L_1$, (A9) reduces to

$$\begin{aligned} h^{(0)}(\mathbf{x}, t) &= \frac{2}{L_1} \sum_{m=1}^{\infty} \frac{\sin(\alpha_m x_1)}{\alpha_m} \left[(H_{10} - (-1)^m H_{20}) e^{-\frac{T_G}{S}\alpha_m^2 t} \right. \\ &\quad \left. + (H_1 - (-1)^m H_2) \left(1 - e^{-\frac{T_G}{S}\alpha_m^2 t}\right) \right]. \end{aligned} \quad (\text{A10})$$

For boundary conditions other than those shown in (5a)-(5d), transformations similar to (A2) can be used upon replacing with appropriate kernels [Özişik, 1989].

Appendix B: Head Perturbation $h'(\mathbf{x}, t)$

The equation for the head perturbation $h'(\mathbf{x}, t)$ reads as

$$\frac{\partial^2 h^{(1)}(\mathbf{x}, t)}{\partial x_i^2} + \frac{\partial}{\partial x_i} \left(Y'(\mathbf{x}) \frac{\partial h^{(0)}(\mathbf{x}, t)}{\partial x_i} \right) = \frac{S}{T_G} \frac{\partial h^{(1)}(\mathbf{x}, t)}{\partial t} \quad (\text{B1})$$

with boundary conditions and initial conditions, as shown in (11). Similarly, using an integral transformation [Özişik, 1989]:

$$h^*(\alpha_m, \beta_n, t) = \int_{\Omega} K(\alpha_m, x_1) K(\beta_n, x_2) h^{(1)}(\mathbf{x}, t) d\mathbf{x}, \quad (\text{B2})$$

where kernels are given in (A3)-(A4), (B1) is transformed to a first-order ordinary differential equation,

$$\frac{dh^*(\alpha_m, \beta_n, t)}{dt} + \frac{T_G}{S} (\alpha_m^2 + \beta_n^2) h^*(\alpha_m, \beta_n, t) = A(\alpha_m, \beta_n, t), \quad (\text{B3})$$

with the initial condition $F^*(\alpha_m, \beta_n) = \int_{\Omega} K(\alpha_m, x_1) K(\beta_n, x_2) H'_0(\mathbf{x}) d\mathbf{x}$. The solution of (B3) can be formally expressed as:

$$h^*(\alpha_m, \beta_n, t) = F^*(\alpha_m, \beta_n) + \int_{t'=0}^t e^{\frac{T_G}{S}(\alpha_m^2 + \beta_n^2)t'} A(\alpha_m, \beta_n, t') dt' \quad (\text{B4})$$

and the solution for $h^{(1)}(\mathbf{x}, t)$ can be derived from the back-transformation of $h^*(\alpha_m, \beta_n, t)$:

$$h^{(1)}(\mathbf{x}, t) = \sum_{m=1}^{\infty} \sum_{n=0}^{\infty} e^{-\frac{T_G}{S}(\alpha_m^2 + \beta_n^2)t} K(\alpha_m, x_1) K(\beta_n, x_2) h^*(\alpha_m, \beta_n, t). \quad (\text{B5})$$

The term on the right-hand side of (B3) is related to boundary conditions for $h^{(1)}$ and the source term, i.e., the second term on the left-hand side of (B1),

$$A(\alpha_m, \beta_n, t) = \frac{T_G}{S} \int_{\Omega} K(\alpha_m, x_1) K(\beta_n, x_2) \frac{\partial}{\partial x_i} \left(Y'(\mathbf{x}) \frac{\partial h^{(0)}(\mathbf{x}, t)}{\partial x_i} \right) d\mathbf{x} \quad (\text{B6})$$

Substituting $h^{(0)}(\mathbf{x}, t)$ into (B6) and carrying out intergration yields

$$\begin{aligned} A(\alpha_m, \beta_n, t) &= \frac{2J_1 T_G \alpha_m}{\sqrt{L_1 L_2} S} \int_{\Omega} Y'(\mathbf{x}') \cos(\alpha_m x'_1) \cos(\beta_n x'_2) d\mathbf{x}' \\ &\quad - \frac{4T_G \alpha_m}{L_1 \sqrt{L_1 L_2} S} \sum_{k=1}^{\infty} b_k e^{-\frac{T_G}{S} \alpha_k^2 t} \int_{\Omega} Y'(\mathbf{x}') \cos(\alpha_m x'_1) \cos(\alpha_k x'_1) \cos(\beta_n x'_2) d\mathbf{x}' \end{aligned} \quad (\text{B7})$$

for $n \neq 0$ and

$$A(\alpha_m, \beta_0, t) = \frac{\sqrt{2}J_1 T_G \alpha_m}{\sqrt{L_1 L_2} S} \int_{\Omega} Y'(\mathbf{x}') \cos(\alpha_m x'_1) d\mathbf{x}' \\ - \frac{2\sqrt{2}T_G \alpha_m}{L_1 \sqrt{L_1 L_2} S} \sum_{k=1}^{\infty} b_k e^{-\frac{T_G}{S} \alpha_k^2 t} \int_{\Omega} Y'(\mathbf{x}') \cos(\alpha_m x'_1) \cos(\alpha_k x'_1) d\mathbf{x}', \quad (\text{B8})$$

for $n = 0$. Substituting $A(\alpha_m, \beta_n, t)$ and $F^*(\alpha_m, \beta_n)$ into (B4) and combining the latter with (B5), one obtains the solution for $h^{(1)}(\mathbf{x}, t)$:

$$h^{(1)}(\mathbf{x}, t) \\ = \frac{4}{D} \sum_{\substack{m=1 \\ n=0}}^{\infty} a_n \sin(\alpha_m x_1) \cos(\beta_n x_2) e^{-\frac{T_G}{S}(\alpha_m^2 + \beta_n^2)t} \int_{\Omega} H'_0(\mathbf{x}') \sin(\alpha_m x'_1) \cos(\beta_n x'_2) d\mathbf{x}' \\ + \frac{4J_1}{D} \sum_{\substack{m=1 \\ n=0}}^{\infty} \frac{a_n \alpha_m \sin(\alpha_m x_1) \cos(\beta_n x_2)}{\alpha_m^2 + \beta_n^2} \left[1 - e^{-\frac{T_G}{S}(\alpha_m^2 + \beta_n^2)t} \right] \int_{\Omega} Y'(\mathbf{x}') \cos(\alpha_m x'_1) \cos(\beta_n x'_2) d\mathbf{x}' \\ - \frac{8T_G}{DL_1 S} \sum_{\substack{m,k=1 \\ n=0}}^{\infty} a_n b_k P_{kmn}(t) \alpha_m \sin(\alpha_m x_1) \cos(\beta_n x_2) \int_{\Omega} Y'(\mathbf{x}') \cos(\alpha_m x'_1) \cos(\alpha_k x'_1) \cos(\beta_n x'_2) d\mathbf{x}' \quad (\text{B9})$$

where $D = L_1 L_2$, $a_n = 1$ for $n \geq 1$ and $a_n = 1/2$ for $n = 0$, and

$$P_{kmn}(t) = \begin{cases} \frac{S}{T_G} \frac{e^{-\frac{T_G}{S} \alpha_k^2 t} - e^{-\frac{T_G}{S}(\alpha_m^2 + \beta_n^2)t}}{\alpha_m^2 + \beta_n^2 - \alpha_k^2}, & \text{if } \alpha_k^2 \neq \alpha_m^2 + \beta_n^2, \\ t e^{-\frac{T_G}{S}(\alpha_m^2 + \beta_n^2)t}, & \text{if } \alpha_k^2 = \alpha_m^2 + \beta_n^2. \end{cases} \quad (\text{B10})$$

The steady state solution of the head perturbation can be derived by taking the limit of (B9) as $t \rightarrow \infty$,

$$h^{(1)}(\mathbf{x}, \infty) = \frac{4J_1}{D} \sum_{\substack{m=1 \\ n=0}}^{\infty} \frac{a_n \alpha_m \sin(\alpha_m x_1) \cos(\beta_n x_2)}{\alpha_m^2 + \beta_n^2} \int_{\Omega} Y'(\mathbf{x}') \cos(\alpha_m x'_1) \cos(\beta_n x'_2) d\mathbf{x}' \quad (\text{B11})$$

Appendix C: Head Covariance

Multiplying $h^{(1)}(\mathbf{y}, \tau)$ to (B9) and taking ensemble mean yields an expression for head covariance

$$\begin{aligned}
C_h(\mathbf{x}, t; \mathbf{y}, \tau) &= \langle h^{(1)}(\mathbf{x}, t) h^{(1)}(\mathbf{y}, \tau) \rangle \\
&= \frac{4}{D} \sum_{\substack{m=1 \\ n=0}}^{\infty} a_n \sin(\alpha_m x_1) \cos(\beta_n x_2) e^{-\frac{T_G}{S}(\alpha_m^2 + \beta_n^2)t} \int_{\Omega} \langle H'_0(\mathbf{x}') h^{(1)}(\mathbf{y}, \tau) \rangle \sin(\alpha_m x'_1) \cos(\beta_n x'_2) d\mathbf{x}' \\
&+ \frac{4J_1}{D} \sum_{\substack{m=1 \\ n=0}}^{\infty} \frac{a_n \alpha_m \sin(\alpha_m x_1) \cos(\beta_n x_2)}{\alpha_m^2 + \beta_n^2} \left[1 - e^{-\frac{T_G}{S}(\alpha_m^2 + \beta_n^2)t} \right] \int_{\Omega} C_{Yh}(\mathbf{x}'; \mathbf{y}, \tau) \cos(\alpha_m x'_1) \cos(\beta_n x'_2) d\mathbf{x}' \\
&- \frac{8T_G}{DL_1 S} \sum_{\substack{m,k=1 \\ n=0}}^{\infty} a_n b_k P_{kmn}(t) \alpha_m \sin(\alpha_m x_1) \cos(\beta_n x_2) \int_{\Omega} C_{Yh}(\mathbf{x}'; \mathbf{y}, \tau) \cos(\alpha_m x'_1) \cos(\alpha_k x'_1) \cos(\beta_n x'_2) d\mathbf{x}'
\end{aligned} \tag{C1}$$

Here the cross-covariance between head at space-time (\mathbf{y}, τ) and initial head at location \mathbf{x} , $\langle H'_0(\mathbf{x}) h^{(1)}(\mathbf{y}, \tau) \rangle$, can be derived by rewriting (B9) in terms of (\mathbf{y}, τ) , multiplying $H'_0(\mathbf{x}')$ to the derived equation, and taking the mean,

$$\begin{aligned}
C_{H_0h}(\mathbf{x}; \mathbf{y}, \tau) &= \langle H_0(\mathbf{x}) h^{(1)}(\mathbf{y}, \tau) \rangle \\
&= \frac{4}{D} \sum_{\substack{m=1 \\ n=0}}^{\infty} a_n \sin(\alpha_m y_1) \cos(\beta_n y_2) e^{-\frac{T_G}{S}(\alpha_m^2 + \beta_n^2)\tau} \int_{\Omega} C_{H_0}(\mathbf{x}', \mathbf{x}) \sin(\alpha_m x'_1) \cos(\beta_n x'_2) d\mathbf{x}' \\
&+ \frac{4J_1}{D} \sum_{\substack{m=1 \\ n=0}}^{\infty} \frac{a_n \alpha_m \sin(\alpha_m y_1) \cos(\beta_n y_2)}{\alpha_m^2 + \beta_n^2} \left[1 - e^{-\frac{T_G}{S}(\alpha_m^2 + \beta_n^2)\tau} \right] \int_{\Omega} C_{YH_0}(\mathbf{x}', \mathbf{x}) \cos(\alpha_m x'_1) \cos(\beta_n x'_2) d\mathbf{x}' \\
&- \frac{8T_G}{DL_1 S} \sum_{\substack{m,k=1 \\ n=0}}^{\infty} a_n b_k P_{kmn}(\tau) \alpha_m \sin(\alpha_m y_1) \cos(\beta_n y_2) \int_{\Omega} C_{YH_0}(\mathbf{x}', \mathbf{x}) \cos(\alpha_m x'_1) \cos(\alpha_k x'_1) \cos(\beta_n x'_2) d\mathbf{x}'
\end{aligned} \tag{C2}$$

As mentioned early, we assume that the flow is initially at a steady state and the perturbation of the initial head $H'_0(x)$ is determined from the steady state condition. Therefore, $C_{YH_0}(\mathbf{x}', \mathbf{x})$ and $C_{H_0}(\mathbf{x}', \mathbf{x})$ can be obtained by replacing J_1 in (15) and (18) by J_0 , the initial hydraulic gradient. Substituting C_{YH_0} and C_{H_0} into (C2) and carrying out integrations, one

has

$$\begin{aligned}
C_{H_0h}(\mathbf{x}; \mathbf{y}, \tau) &= \langle H_0(\mathbf{x}) h^{(1)}(\mathbf{y}, \tau) \rangle \\
&= \frac{16J_0}{D^2} \sum_{\substack{m, m_1=1 \\ n, n_1=0}}^{\infty} \frac{a_n a_{n_1} \alpha_m \alpha_{m_1} Q_{m_1 n_1}^{mn} SC}{(\alpha_m^2 + \beta_n^2)(\alpha_{m_1}^2 + \beta_{n_1}^2)} J_{mn}(\tau) \\
&\quad - \frac{32J_0 T_G}{D^2 L_1 S} \sum_{\substack{m, m_1, k=1 \\ n, n_1=0}}^{\infty} \frac{a_n a_{n_1} b_k P_{kmn}(\tau) \alpha_m \alpha_{m_1} Q_{m_1 n_1}^{kmn} SC}{(\alpha_{m_1}^2 + \beta_{n_1}^2)} \quad (C3)
\end{aligned}$$

where

$$SC = \sin(\alpha_m y_1) \cos(\beta_n y_2) \sin(\alpha_{m_1} x_1) \cos(\beta_{n_1} x_2), \quad (C4)$$

$$J_{mn}(\tau) = \left[J_1 + (J_0 - J_1) e^{-\frac{T_G}{S}(\alpha_m^2 + \beta_n^2)\tau} \right], \quad (C5)$$

$$\begin{aligned}
R_{m_1 n_1}(\mathbf{x}) &= \int_{\Omega} C_Y(\mathbf{x}, \mathbf{x}') \cos(\alpha_{m_1} x'_1) \cos(\beta_{n_1} x'_2) d\mathbf{x}' \\
&= \frac{\lambda_1 \lambda_2 \sigma_Y^2}{(\alpha_{m_1}^2 \lambda_1^2 + 1)(\beta_{n_1}^2 \lambda_2^2 + 1)} \left[2 \cos(\alpha_{m_1} x_1) - e^{-x_1/\lambda_1} - (-1)^{m_1} e^{(x_1 - L_1)/\lambda_1} \right] \\
&\quad \left[2 \cos(\beta_{n_1} x_2) - e^{-x_2/\lambda_2} - (-1)^{n_1} e^{(x_2 - L_2)/\lambda_2} \right] \quad (C6)
\end{aligned}$$

$$\begin{aligned}
Q_{m_1 n_1}^{mn} &= \int_{\Omega} R_{m_1 n_1}(\mathbf{x}) \cos(\alpha_m x_1) \cos(\beta_n x_2) d\mathbf{x} \\
&= \frac{\lambda_1 \lambda_2 \sigma_Y^2}{(\alpha_{m_1}^2 \lambda_1^2 + 1)(\beta_{n_1}^2 \lambda_2^2 + 1)} \left[L_1 \delta_{mm_1} + \frac{\lambda_1}{\alpha_m^2 \lambda_1^2 + 1} (1 + (-1)^{m+m_1}) ((-1)^m e^{-L_1/\lambda_1} - 1) \right] \\
&\quad \left[L_2 (\delta_{nn_1} + \delta_{n0} \delta_{n_1 0}) + \frac{\lambda_2}{\beta_n^2 \lambda_2^2 + 1} (1 + (-1)^{n+n_1}) ((-1)^n e^{-L_2/\lambda_2} - 1) \right] \quad (C7)
\end{aligned}$$

$$\begin{aligned}
Q_{m_1 n_1}^{kmn} &= \int_{\Omega} R_{m_1 n_1}(\mathbf{x}) \cos(\alpha_k x_1) \cos(\alpha_m x_1) \cos(\beta_n x_2) d\mathbf{x} \\
&= \frac{\lambda_1 \lambda_2 \sigma_Y^2}{2(\alpha_{m_1}^2 \lambda_1^2 + 1)(\beta_{n_1}^2 \lambda_2^2 + 1)} \left[L_1 (\delta_{m_1, m+k} + \delta_{m, m_1+k} + \delta_{k, m+m_1}) \right. \\
&\quad \left. + \lambda_1 (\eta_{mk}^- + \eta_{mk}^+) (1 + (-1)^{m+m_1}) ((-1)^m e^{-L_1/\lambda_1} - 1) \right] \\
&\quad \left[L_2 (\delta_{nn_1} + \delta_{n0} \delta_{n_1 0}) + \frac{\lambda_2}{\beta_n^2 \lambda_2^2 + 1} (1 + (-1)^{n+n_1}) ((-1)^n e^{-L_2/\lambda_2} - 1) \right] \quad (C8)
\end{aligned}$$

and $\eta_{mk}^- = [(\alpha_m - \alpha_k)^2 \lambda_1^2 + 1]^{-1}$, $\eta_{mk}^+ = [(\alpha_m + \alpha_k)^2 \lambda_1^2 + 1]^{-1}$.

Similarly, the cross-covariance $C_{Yh}(\mathbf{x}'; \mathbf{y}, \tau) = \langle Y'(\mathbf{x}) h^{(1)}(\mathbf{y}, \tau) \rangle$ can be derived as

$$\begin{aligned}
C_{Yh}(\mathbf{x}; \mathbf{y}, \tau) &= \frac{4}{D} \sum_{\substack{m=1 \\ n=0}}^{\infty} \frac{a_n \alpha_m \sin(\alpha_m y_1) \cos(\beta_n y_2)}{\alpha_m^2 + \beta_n^2} R_{mn}(\mathbf{x}) J_{mn}(\tau) \\
&- \frac{8T_G}{DL_1 S} \sum_{\substack{m,k=1 \\ n=0}}^{\infty} a_n b_k P_{kmn}(\tau) \alpha_m \sin(\alpha_m y_1) \cos(\beta_n y_2) R_{kmn}(\mathbf{x}) \quad (C9)
\end{aligned}$$

where

$$\begin{aligned}
R_{kmn}(\mathbf{x}) &= \int_{\Omega} C_Y(\mathbf{x}', \mathbf{x}) \cos(\alpha_m x'_1) \cos(\alpha_k x'_1) \cos(\beta_n x'_2) d\mathbf{x}' \\
&= \frac{\lambda_1 \lambda_2 \sigma_Y^2}{2(\beta_n^2 \lambda_2^2 + 1)} \left\{ 2 \eta_{mk}^+ \cos[(\alpha_m + \alpha_k) x_1] + 2 \eta_{mk}^- \cos[(\alpha_m - \alpha_k) x_1] \right. \\
&\quad \left. - (\eta_{mk}^+ + \eta_{mk}^-) [e^{-x_1/\lambda_1} + (-1)^m e^{(x_1-L_1)/\lambda_1}] \right\} \\
&\quad \times [2 \cos(\beta_n x_2) - e^{-x_2/\lambda_2} - (-1)^n e^{(x_2-L_2)/\lambda_2}] \quad (C10)
\end{aligned}$$

After substituting $C_{H_0h}(\mathbf{x}; \mathbf{y}, \tau)$ and $C_{Yh}(\mathbf{x}; \mathbf{y}, \tau)$ into (C1) and carrying out integrations gives

$$\begin{aligned}
C_h(\mathbf{x}, t; \mathbf{y}, \tau) &= \frac{16}{D^2} \sum_{\substack{m,m_1=1 \\ n,n_1=0}}^{\infty} \frac{a_n a_{n_1} \alpha_m \alpha_{m_1} Q_{mn}^{m_1 n_1} SC}{(\alpha_m^2 + \beta_n^2)(\alpha_{m_1}^2 + \beta_{n_1}^2)} J_{mn}(t) J_{m_1 n_1}(\tau) \\
&- \frac{32T_G}{D^2 L_1 S} \sum_{\substack{m,m_1,k_1=1 \\ n,n_1=0}}^{\infty} \frac{a_n a_{n_1} \alpha_m \alpha_{m_1} b_{k_1} P_{k_1 m_1 n_1}(\tau) SC}{\alpha_m^2 + \beta_n^2} Q_{mn}^{k_1 m_1 n_1} J_{mn}(t) \\
&- \frac{32T_G}{D^2 L_1 S} \sum_{\substack{m,m_1,k=1 \\ n,n_1=0}}^{\infty} \frac{a_n a_{n_1} \alpha_m \alpha_{m_1} b_k P_{kmn}(t) SC}{\alpha_{m_1}^2 + \beta_{n_1}^2} Q_{m_1 n_1}^{kmn} J_{m_1 n_1}(\tau) \\
&+ \frac{64T_G^2}{D^2 L_1^2 S^2} \sum_{\substack{m,m_1,k,k_1=1 \\ n,n_1=0}}^{\infty} a_n a_{n_1} \alpha_m \alpha_{m_1} b_k b_{k_1} P_{kmn}(t) P_{k_1 m_1 n_1}(\tau) SC Q_{kmn}^{k_1 m_1 n_1} \quad (C11)
\end{aligned}$$

where

$$\begin{aligned}
Q_{kmn}^{k_1 m_1 n_1} &= \int_{\Omega} R_{kmn}(\mathbf{x}) \cos(\alpha_{k_1} x_1) \cos(\alpha_{m_1} x_1) \cos(\beta_{n_1} x_2) d\mathbf{x} \\
&= \frac{\lambda_1 \lambda_2 \sigma_Y^2}{4(\beta_n^2 \lambda_2^2 + 1)} \left[L_1 \eta_{mk}^+ (\delta_{m+k, m_1+k_1} + \delta_{k_1, m+k+m_1} + \delta_{m_1, m+k+k_1}) \right. \\
&\quad + L_1 \eta_{mk}^- (\delta_{k, m+m_1+k_1} + \delta_{m, k+m_1+k_1} + \delta_{m+m_1, k+k_1} + \delta_{m+k_1, m_1+k}) \\
&\quad + \lambda_1 (\eta_{mk}^- + \eta_{mk}^+) (\eta_{m_1 k_1}^- + \eta_{m_1 k_1}^+) (1 + (-1)^{m+k}) ((-1)^{m_1+k_1} e^{-L_1/\lambda_1} - 1) \Big] \\
&\quad \left[L_2 (\delta_{nn_1} + \delta_{n0} \delta_{n_1 0}) + \frac{\lambda_2}{\beta_{n_1}^2 \lambda_2^2 + 1} (1 + (-1)^{n+n_1}) ((-1)^{n_1} e^{-L_2/\lambda_2} - 1) \right]
\end{aligned} \tag{C12}$$

In particular, letting $t = \infty$ and $\tau = \infty$, we obtain the steady state head variance

$$C_h(\mathbf{x}; \mathbf{y}) = \frac{16J_1^2}{D^2} \sum_{\substack{m, m_1=1 \\ n, n_1=0}}^{\infty} \frac{a_n a_{n_1} \alpha_m \alpha_{m_1} Q_{mn}^{m_1 n_1} S C}{(\alpha_m^2 + \beta_n^2)(\alpha_{m_1}^2 + \beta_{n_1}^2)} \tag{C13}$$

LIST OF REFERENCES

- Dagan G., Models of groundwater flow in statistically homogeneous porous formations, *Water Resour. Res.*, 15(1), 47-63, 1979.
- Dagan G., Stochastic modeling of groundwater flow by unconditional and conditional probabilities, 1. Conditional simulation and the direct problem, *Water Resour. Res.*, 18(4), 813-833, 1982.
- Dagan G., Stochastic modeling of groundwater flow by unconditional and conditional probabilities: The inverse problem, *Water Resour. Res.*, 21(1), 65-72, 1985.
- Dagan G., Flow and Transport in Porous Formations, Springer, New York, 1989.
- Dettinger, M. D., and J. Wilson, First-order analysis of uncertainty in numerical models of groundwater flow, 1. Mathematical development, *Water Resour. Res.*, 17(1), 149-161, 1981.
- Freeze, R.A., A stochastic-conceptual analysis of one-dimensional groundwater flow in nonuniform homogeneous media, *Water Resour. Res.*, 11(5), 725-741, 1975.
- Gelhar, L. W., and C. L. Axness, Three-dimensional stochastic analysis of macrodispersion in aquifers, *Water Resour. Res.*, 19(1), 161-180, 1983.
- Guadagnini, A., and S. P. Neuman, Nonlocal and localized analyses of conditional mean steady state flow in bounded, randomly nonuniform domains, 1, Theory and computational approach, *Water Resour. Res.*, 35(10), 2999-3018, 1999a.
- Guadagnini, A., and S. P. Neuman, Nonlocal and localized analyses of conditional mean steady state flow in bounded, randomly nonuniform domains, 2, computational examples, *Water Resour. Res.*, 35(10), 3019-3039, 1999b.
- Gutjahr, A. L., and L. W. Gelhar, Stochastic models of subsurface flow: Infinite versus finite domains and stationarity, *Water Resour. Res.*, 17(2), 337-350, 1981.

- Mizell, S. A., A. L. Gutjahr, and L. W. Gelhar, Stochastic analysis of spatial variability in two-dimensional steady groundwater flow assuming stationary and nonstationary heads, *Water Resour. Res.*, 18, 1053-1067, 1982.
- Neuman S. P., and S. Orr, Prediction of steady state flow in nonuniform geologic media by conditional moments: exact nonlocal formalism, effective conductivities, and weak approximation, *Water Resour. Res.*, 29, 341-364, 1993.
- Osnes H., Stochastic analysis of head spatial variability in bounded rectangular heterogeneous aquifers, *Water Resour. Res.*, 31(12), 2981-2990, 1995.
- Osnes H., Stochastic analysis of velocity spatial variability in bounded rectangular heterogeneous aquifers, *Advances in Water Resour.*, 21, 203-215, 1998.
- Rubin Y., and G. Dagan, Stochastic analysis of boundary effects on head spatial variability in heterogeneous aquifers, 1. Constant head boundary, *Water Resour. Res.*, 24, 1689-1697, 1988.
- Rubin Y., and G. Dagan, Stochastic analysis of boundary effects on head spatial variability in heterogeneous aquifers, 2. Impervious boundary, *Water Resour. Res.*, 25, 707-712, 1989.
- Rubin Y., and G. Dagan, A note on head and velocity covariances in three-dimensional flow through heterogeneous anisotropic porous media, *Water Resour. Res.*, 28(5), 1463-1470, 1992.
- Smith, L., and R. A. Freeze, Stochastic analysis of steady state groundwater flow in a bounded domain, 2. Two-dimensional simulations, *Water Resour. Res.*, 15(6), 1543-1559, 1979.
- Tartakovsky, D. M., and I. Mitkov, Some aspects of head-variance evaluation, *Comput. Geosci.*, 3, 89-92, 1999.
- Tartakovsky, D., and S.P. Neuman, Transient flow in bounded randomly heterogeneous domains, 1. Exact conditional moment equations and recursive approximations, *Water Resour. Res.*, 34(1), 1-12, 1998.

- Zhang, D., and S. P. Neuman, Comments on ‘A note on head and velocity covariances in three-dimensional flow through heterogeneous anisotropic porous media” by Y. Yubin and G. Dagan, *Water Resour. Res.*, 28(12), 3343-3344, 1992.
- Zyvoloski, G. A., B. A. Robinson, Z. V. Dash, and L. L. Trease, Summary of the models and methods for the FEHM application—A Finite-Element Heat- and Mass-Transfer code, LA-13307-MS, Los Alamos National Laboratory, 1997.

Figure Captions

Figure 1 Transient mean head computed using different numbers of terms, N , in truncating infinite series in (7): the base case.

Figure 2 Transient head variance computed using different numbers of terms, N , in truncating infinite series in (22): the base case.

Figure 3 Transient head variance computed using different numbers of terms in truncating infinite series in (22): $L_2 = 2.0$.

Figure 4 Transient head variance computed using different numbers of terms in truncating infinite series in (22): $\lambda_1 = \lambda_2 = 2.0$.

Figure 5 Comparisons of (a) the transient mean head and (b) the transient head variance computed from Monte Carlo simulations (solid curves), the first-order analytical solution (dashed curves), and the first-order moment-equation method (dash-dotted curves).

Figure 6 The transient cross-covariance (a) between the log transmissivity $Y(x_1, L_2/2)$ and the hydraulic head $h(x_1, L_2/2, t)$, and (b) between the log transmissivity $Y(L_1/2, L_2/2)$ and the hydraulic head $h(x_1, L_2/2, t)$.

Figure 7 The transient head covariance between head $h(\mathbf{x}, t)$ and $h(\mathbf{x}, \tau)$ as a function of x_1 and time τ along $x_2 = L_2/2$ for (a) $t = 0.0$, and (b) $t = 0.05$.

Figure 8 Comparisons of the transient mean longitudinal flux computed from Monte Carlo simulations (solid curves), the first-order analytical solution (dashed curves), and the first-order moment-equation method (dash-dotted curves).

Figure 9 Comparisons of (a) the longitudinal flux variance and (b) the transverse flux variance computed from Monte Carlo simulations (solid curves), the first-order analytical solution (dashed curves), and the first-order moment-equation method (dash-dotted curves).

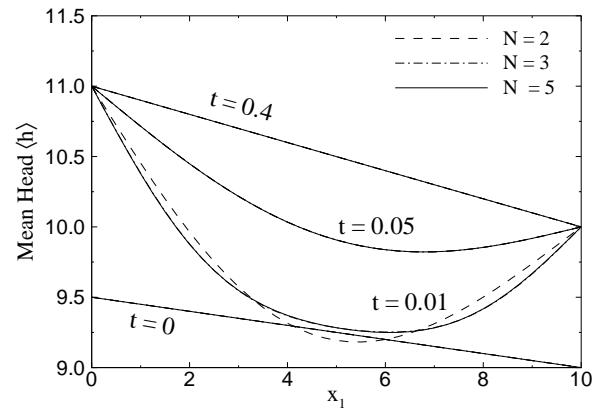


Figure 1:

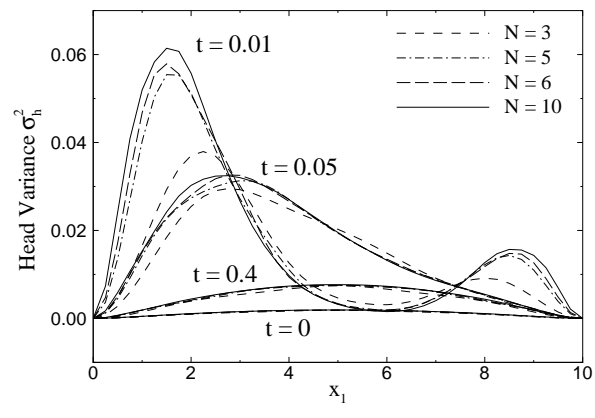


Figure 2:

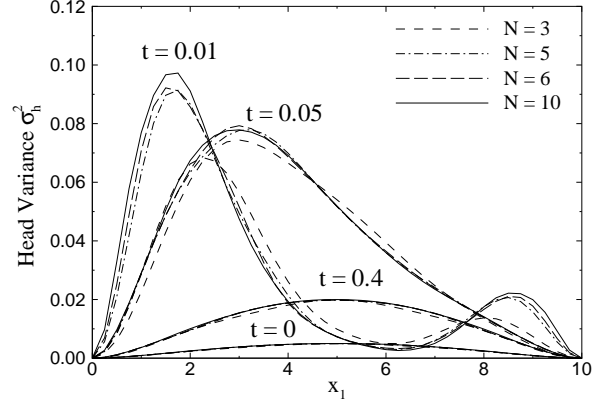


Figure 3:

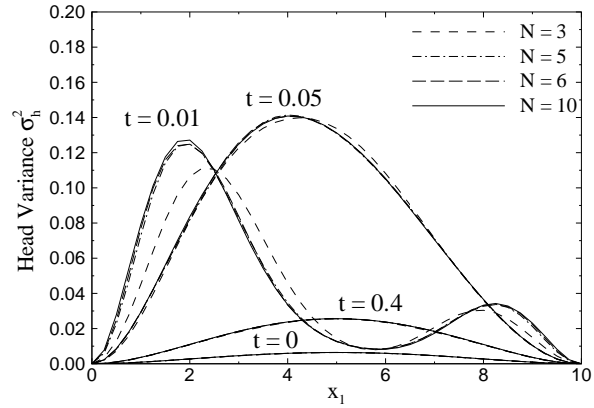


Figure 4:

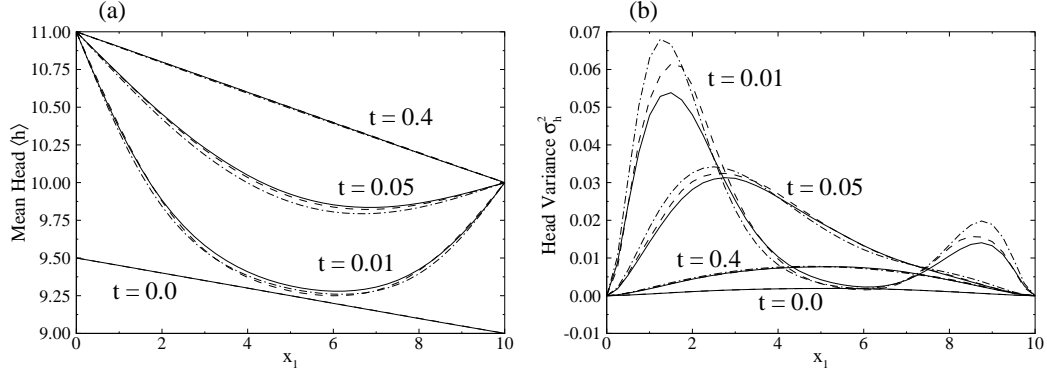


Figure 5:

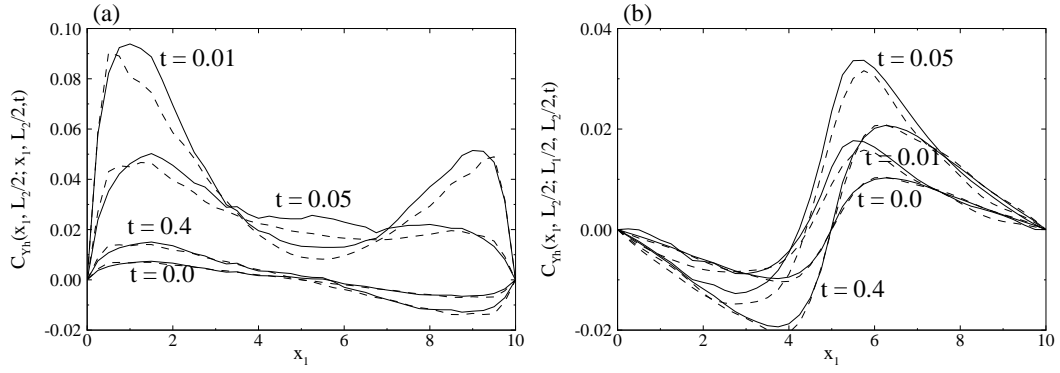


Figure 6:

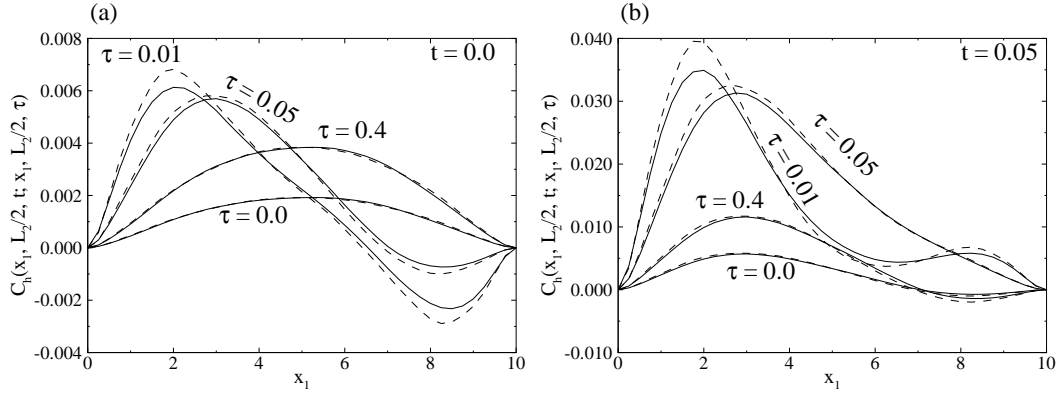


Figure 7:

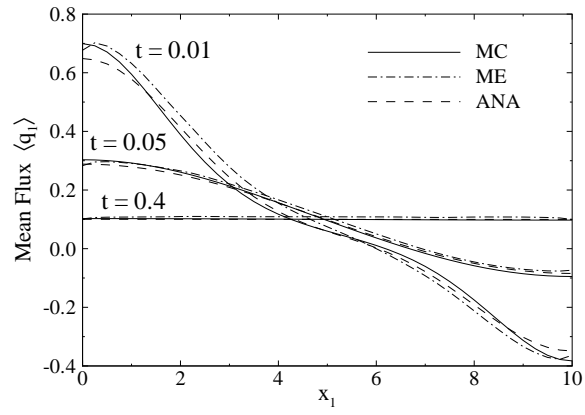


Figure 8:

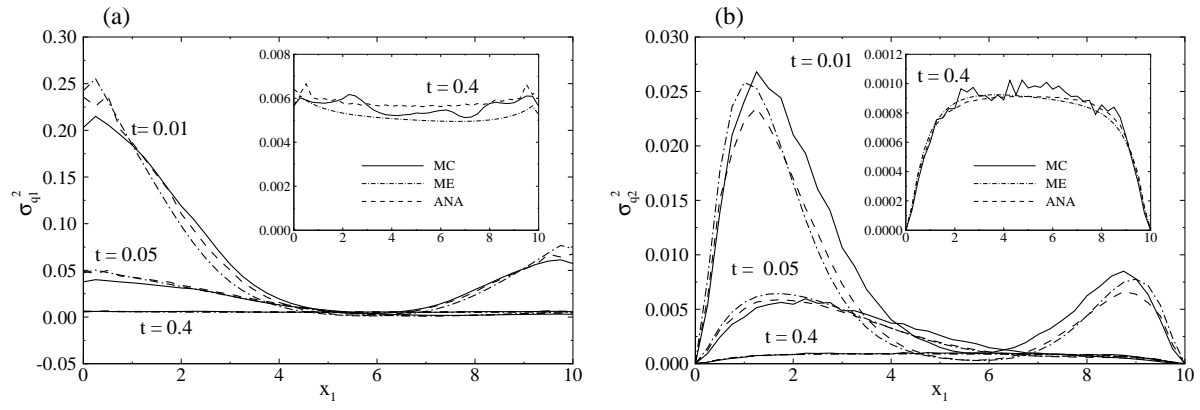


Figure 9: